J Mol Model (2010) 16:337–342
DOI 10.1007/s00894-009-0545-7

ORIGINAL PAPER

Theoretical description of bonding in *cis*-$W(CO)_4(piperidine)_2$ and its dimer

Mariusz P. Mitoraj · Artur Michalak

Received: 22 May 2009 / Accepted: 9 June 2009 / Published online: 15 July 2009

Abstract The gradient-corrected DFT calculations were applied to characterize the bonding in the *cis*-$W(CO)_4(piperidine)_2$ complex and its dimer. The Nalewajski–Mrozek bond order analysis, the Ziegler–Rauk bond-energy partitioning and Natural Orbitals for Chemical Valence (NOCV's) were applied in a description of the electronic structure of *cis*-$W(CO)_4(piperidine)_2$. The results indicate that the metal-carbon bond *trans* to piperidine is stronger than that in the *cis* position, as a result of an increase in both, the ligand→ metal donation and metal → ligand π-back-bonding; this implies a weakening of the carbon–oxygen bond. In the dimeric complex, modeling the interactions in the solid state, the C–O bond is further weakened resulting in the lowering the CO stretching frequencies, observed experimentally by Braunstein et al. (Angew. Chem. Int. Ed. (2004), 43:5922–5925).

Keywords Bond orders · *Cis*-W(CO)4(piperidine)2 · Deformation density · NOCV

Introduction

As one of the longest-known types of complexes [1], transition-metal carbonyls have been a subject of extensive experimental and theoretical studies, involving numerous experimental techniques and computational methods [2–14]. Carbon monoxide as a ligand plays a special role in inorganic and organometallic chemistry [2–12], as well as in catalysis [13–16]. The carbon–oxygen bond in carbonyl complexes varies between double and triple bond, and practically a smooth transition can be observed for the complexes with different transition-metals and different ligands [2–4, 17, 25]. This makes carbonyl complexes useful for probing the electronic structure of different systems by spectroscopic techniques [2–4, 17].

The CO stretching frequency in isolated carbon monoxide is 2143 cm^{-1}. In the complexes with terminal CO ligands, it is usually in the range 1850–2100 cm^{-1} [2–4, 17]. Recently, exceptionally low IR frequencies, below 1770 cm^{-1}, were observed by Braunstein et al. [18] for the *cis*-$W(CO)_4(piperidine)_2$ complex in the solid state; this was explained by the supramolecular NH–-OC–W hydrogen bonds.

The main purpose of the present work is to characterize bonding in the the *cis*-$W(CO)_4(piperidine)_2$ complex by theoretical (DFT) calculations. This study involves monomeric form of *cis*-$W(CO)_4(piperidine)_2$ complex as well as its dimer (Fig. 1), as a simple model including the interactions present in the solid state. The electronic structure will be analyzed in terms of bond-orders, calculated with the Nalewajski–Mrozek (NM) method, [19–25], bond-energy, and its partitioning according to Ziegler–Rauk analysis [26, 27] and recently proposed natural orbitals for chemical valence (NOCV) [28–33].

Computational details and the model systems

In all the calculations the Amsterdam Density Functional (ADF) program [34–37] was used. The Becke–Perdew exchange-correlation functional [38–40] was applied. A standard double-zeta STO basis with one set of polarization functions was used for main-group elements (H, C, N, O),

M. P. Mitoraj · A. Michalak (✉)
Department of Theoretical Chemistry, Faculty of Chemistry,
Jagiellonian University,
R. Ingardena 3,
30-060 Cracow, Poland
e-mail: michalak@chemia.uj.edu.pl

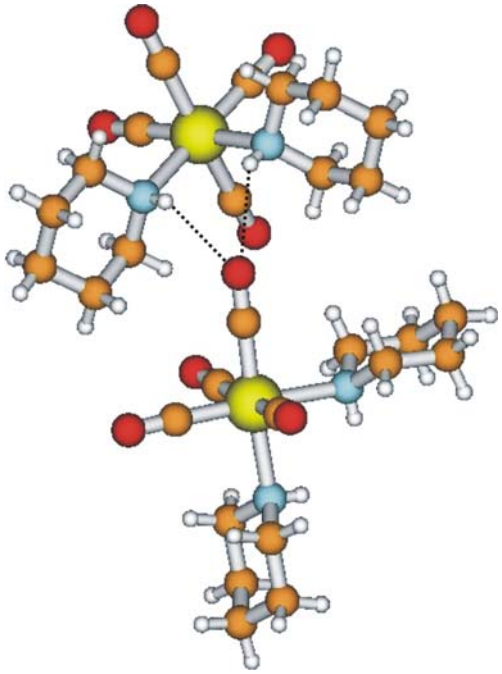

Fig. 1 Interaction of two molecules in the crystal structure of cis-W $(CO)_4$(piperidine)$_2$, involving supramolecular hydrogen bond, N–H—O=C–W [18]

while a standard triple-zeta basis set was employed for tungsten. The *1s* electrons of C, N, O, as well as the *1s–4d* electrons of W were treated as frozen core. Auxiliary *s*, *p*, *d*, *f*, and *g* STO functions, centered on all nuclei, were used to fit the electron density and obtain accurate Coulomb and exchange potentials in each SCF cycle. The reported energy differences include first-order scalar relativistic correction [41–43]. The Nalewajski–Mrozek bond order analysis [19–25], Natural Orbitals for Chemical Valence [28–33], and the Ziegler–Rauk bond-energy decomposition [26, 27] were also used.

The dimeric model extracted from the crystal structure [18] of *cis*-W$(CO)_4$(piperidine)$_2$ complex is shown in Fig. 1. The calculations were performed for this system in the experimental geometry, since it was our intention to analyze the electronic structure of the complex directly corresponding to experimental results from Ref. [18]. The calculations for the *cis*-W$(CO)_4$(piperidine)$_2$ monomer were carried out for the experimental (crystal structure) geometry as well; in addition, the geometry optimization was performed, to investigate the geometry effect on the results.

The Natural Orbitals for Chemical Valence (NOCV) have been derived from the Nalewajski–Mrozek valence theory [19–25]. Let us consider the molecular system A–B, consisting of two molecular fragments A and B (*e.g.*, transition-metal-containing-fragment and the ligand). The molecular wavefunction (electron density) can be expressed in the basis of the fragment orbitals. The deformation density (differential density) can be defined with respect to the fragment densities,

$$\Delta\rho(r) = \rho_{AB}(r) - \rho_A^0(r) - \rho_B^0(r) \tag{1}$$

The NOCV's, ψ_i , are defined as the eigenvectors, $\psi_i = \sum_j^N C_{ij}\chi_j$, that diagonalize the deformation density matrix, $\mathbf{\Delta P}$:

$$\mathbf{\Delta P C_i} = \mathbf{v_i C_i}, \qquad \mathbf{i = 1 \ldots .N} \tag{2}$$

where N denotes the number of basis functions, $\{\chi_j, j=1, N\}$, used in the representation for $\mathbf{\Delta P}$.

The deformation density matrix, $\mathbf{\Delta P}$ is defined as:

$$\mathbf{\Delta P = P - P^0} \tag{3}$$

where $\mathbf{P}$ and $\mathbf{P^0}$ correspond to the density matrices of the combined molecule ($\mathbf{P}$) and the considered molecular fragments ($\mathbf{P^0}$). We shall in the following represent ΔP in a basis of orthogonalized fragment Kohn–Sham (KS) orbitals (OFO). In such a basis the NOCV's are the eigenfunctions of ΔP [28–33].

It follows further [28–33] that the deformation density, $\Delta\rho = \rho(\text{molecule}) - \rho^0(\text{fragments})$, can be expressed in the NOCV representation as a sum of pairs of complementary eigenfunctions (ψ_{-k}, ψ_k) corresponding to the eigenvalues v_k and $-v_k$ with the same absolute value but opposite signs:

$$\Delta\rho(r) = \sum_{k=1}^{N/2} v_k\left[-\psi_{-k}^2(r) + \psi_k^2(r)\right] = \sum_{k=1}^{N/2} \Delta\rho_k(r). \tag{4}$$

Here the fact that the eigenvalues appear in pairs, where $v_k = -v_k$, is a consequence of $\mathbf{\Delta P}$ being a traceless matrix expressed in an orthonormal (OFO) basis. In Eq. (4): an eigenvalue v_k corresponds to the fraction of an electron charge that is transferred from the ψ_{-k} orbital to the ψ_k orbital, when the molecule is formed from the fragments. In our study the bonding between carbonyl species $C_{(3)}O_{(8)}$/$C_{(4)}O_{(9)}$ with the metal fragment W$(CO)_3$(pip)$_2$ will be discussed. The subscript in parenthesis corresponds to the labeling as in Fig. 2. The complementary pairs of each NOCV's define a separate channel for electron charge transfer between the molecular fragments [28–31]. The total charge transferred in this channel is:

$$\Delta q_k = v_k. \tag{5}$$

In the present study the Ziegler–Rauk bond-energy decomposition (extended-transition-state, ETS) method [26, 27] was also applied. In this scheme, the total bonding

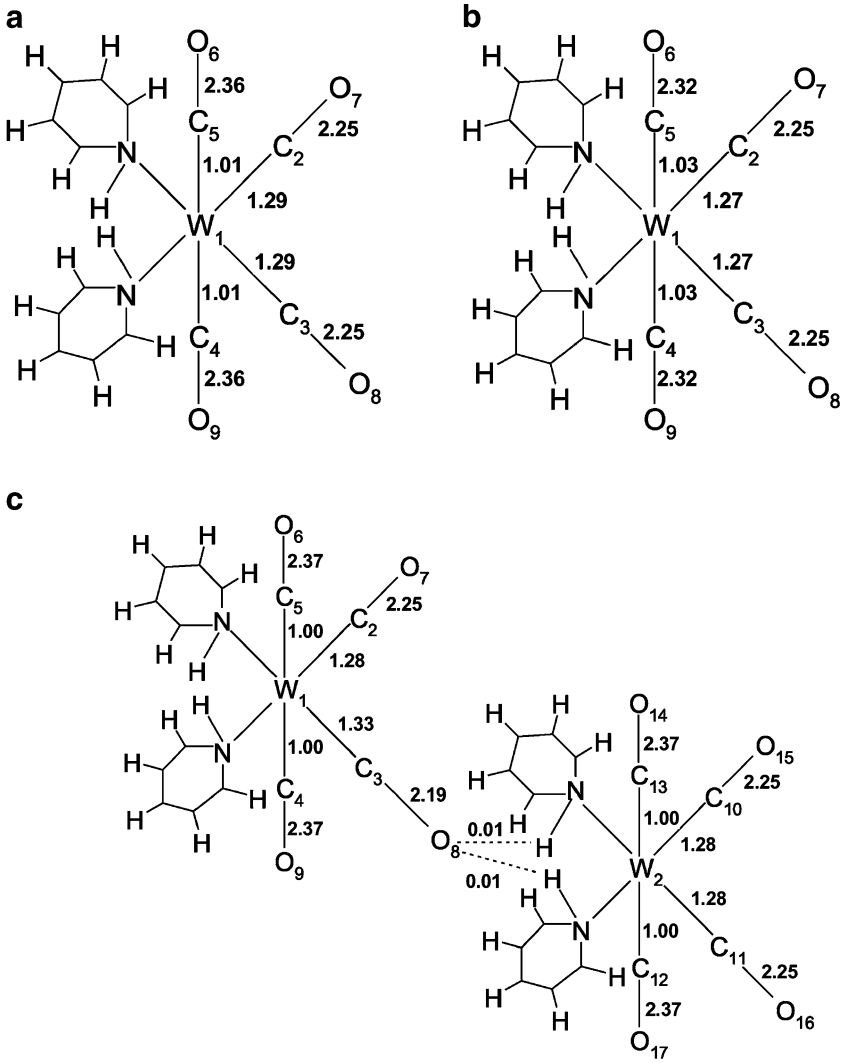

Fig. 2 The tungsten carbon and carbon–oxygen bond orders calculated with Nalewajski–Mrozek method for the *cis*-W$(CO)_4$(piperidine)$_2$ complex (**a** and **b**) and the dimeric system (**c**), extracted from the crystal structure. The results in panel **a** and **c** were obtained from the calculations performed for experimental geometry, while in panel **b**—for the optimized structure

energy (ΔE_{total}) between the interacting fragments is divided into three chemically meaningful components:

$$\Delta E_{total} = \Delta E_{elstat} + \Delta E_{Pauli} + \Delta E_{orb}. \quad (6)$$

The first component, ΔE_{elstat}, corresponds to the classical electrostatic interaction between the promoted fragments as they are brought to their positions in the final complex. The second term, ΔE_{Pauli}, accounts for the repulsive Pauli interaction between occupied orbitals on the two fragments in the combined complex. Finally, the last contribution, ΔE_{orb}, represents the stabilizing interactions between the occupied molecular orbitals on one fragment with the unoccupied molecular orbitals of the other fragment as well as mixing of occupied and virtual orbitals within the same fragment (intra-fragment polarization) after the two fragments have been united. The total bonding energy of Eq. (6) refers to the fragments A and B in the same geometry as in the whole system A–B. It should be emphasized here that in the present study we apply the sign-convention that is usually used in connection with the ETS method; namely, the negative/positive sign of the bond energy (component) corresponds to the stabilizing/destabilizing contribution.

Results and discussion

Let us start the discussion with bond-orders in the monomeric *cis*-W$(CO)_4$(piperidine)$_2$ complex. Figure 2(a and b) displays the tungsten-carbon and carbon-carbon bond-orders calculated with Nalewajski–Mrozek method. An asymmetry in bond-orders characterizing the bonds in the positions *cis* and *trans* to piperidine is clearly seen. The W–C bonds *trans* to piperidine are substantially stronger (1.29, 1.27, for experimental and optimized geometry, respectively) than those in the position *trans* to CO (1.01 and 1.03). The trend in corresponding C–O bonds is opposite: these in the position *trans* to piperidine are

slightly weaker (2.25) than those in the *cis* position (2.36 and 2.32). Thus, the presence of the piperidine ligand is partly responsible for weakening of the CO bonds, that is reflected by lowering the CO stretching frequencies in the IR experiments [18]. It should be pointed out that the changes in the calculated bond-orders are relatively small, of the order of 0.1, and thus, one should be careful with interpretation of results. However, it has been shown previously [25] for d^6 and d^{10} TM-carbonyl complexes that the Nalewajski–Mrozek bond-orders correlate well with experimental CO stretching frequencies; for those complexes it has been found that the change in the bond-multiplicities of the order of 0.1, corresponds to the shift in vibrational frequencies by ca. 60 cm^{-1}.

A comparison of the numbers presented in panels a and b of Fig. 2 shows that the differences in the experimental and optimized geometry have minor influence on the qualitative picture resulting from the calculated bond-orders.

Figure 2c shows the corresponding bond-order values calculated for the dimeric structure, with the same arrangement of the two molecules as in the crystal structure. Compared to the monomer, the bond-order values are practically not changed, except from the bonds directly involved in the interaction of the two molecules. Due to the interaction, the $C_{(3)}$–$O_{(8)}$ bond-order is noticeably decreased in the dimer (2.19) compared to the monomer (2.25). This is accompanied by a slight increase in the corresponding tungsten-carbon (W_1–C_3) bond-order: from 1.29 to 1.33. Thus, formation of the supramolecular hydrogen-bond does indeed result in a decrease in the CO bond-strength [18]. However, it is worth pointing out that this effect is smaller than the influence of the piperidine ligand in the *trans* position.

In order to further characterize the difference in the bond between CO and the tungsten-containing fragment we have calculated the fragment-fragment bond-energy in the monomeric complex for the two bonding situations, when CO is located either in *cis* or in the *trans* position to piperidine. For this complex we have also calculated the natural orbitals for chemical valence to determine the corresponding donation/back donation contributions (Eqs. 4, 5). The results are reported in Table 1 and Fig. 3.

The values of the total bonding energy (ΔE_{total}) of Table 1 show that the organometallic-fragment-CO bond energy is −68.5 kcal mol^{-1} for $C_{(3)}O_{(8)}$ (*trans* to piperidine) and −49.3 kcal mol^{-1} for $C_{(4)}O_{(9)}$ (*trans* to CO). Thus, the difference in the two bond energies is ca. −20 kcal mol^{-1}. This reflects a relatively large difference in the W–C bond-orders (ca. 0.3).

The bond-energy was further decomposed into the orbital, electrostatic, and Pauli repulsion contributions, according to the Ziegler–Rauk energy decomposition

Table 1 The total bonding energy[a], ΔE_{total}, describing the bond between carbonyl ligands, $C_{(3)}O_{(8)}$, $C_{(4)}O_{(9)}$, and the metal containing-fragment, $W(CO)_3(pip)_2$, together with the orbital-interaction energy, ΔE_{orb}, and the donation (Δq_d) and the back-donation (Δq_{bd}) measures (Eq. 4) obtained from the NOCV's. The atoms labeling as in Fig. 2

	$W(CO)_3(pip)_2$–$C_{(3)}O_{(8)}$	$W(CO)_3(pip)_2$–$C_{(4)}O_{(9)}$
ΔE_{total} [a)]	−68.54	−49.34
ΔE_{orb} [a)]	−113.90	−85.9
Δq_d	0.65	0.55
Δq_{bd}	1.09	0.94
$\Delta q_d + \Delta q_{bd}$	1.74	1.49

a) in kcal mol^{-1}, $\Delta E_{total} = \Delta E_{orb} + \Delta E_{steric} = \Delta E_{orb} + \Delta E_{Pauli} + \Delta E_{elstat}$.

analysis [26, 27]. The orbital-interaction energy (ΔE_{orb}), represents the stabilizing interactions between the occupied molecular orbitals on one fragment with the unoccupied molecular orbitals of the other fragment as well as mixing of occupied and virtual orbitals within the same fragment (intra-fragment polarization). We can see from Table 1 that ΔE_{orb} is given by −113.9 kcal mol^{-1} for C_3O_8 (*trans* to piperidine) and −85.9 kcal mol^{-1} for $C_{(4)}O_{(9)}$ (*trans* to CO); the difference in the two terms is ca. −28 kcal mol^{-1}. Thus, the orbital-interaction energy is a dominant contribution, mostly determining the difference in the total bonding energy. The difference in electrostatic and Pauli-repulsion terms is much smaller (ca. 8 kcal mol^{-1}), compensating only part of ΔE_{orb}.

Figure 3 shows the deformation density contributions (Eq. 4) from the complementary pairs of NOCV for the $W(CO)_4(piperidine)_2$ complex. It is clearly seen that the contribution from first and second pairs: (φ_{-1}, φ_1), (φ_{-2}, φ_2)

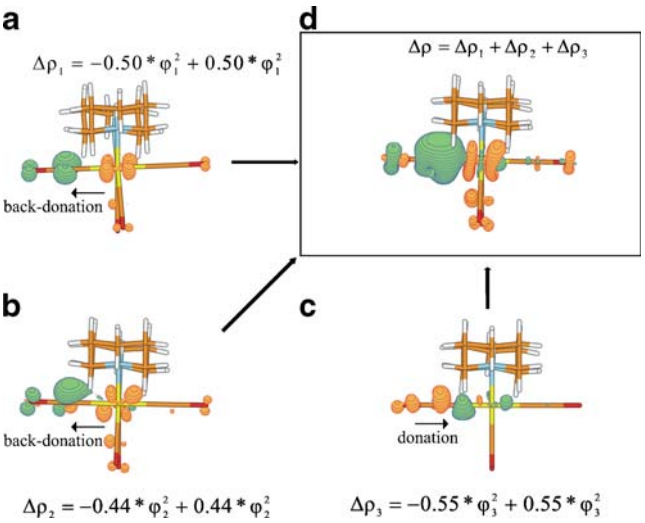

Fig. 3 The back-donation ($\Delta\rho_1$, $\Delta\rho_2$) and donation contributions ($\Delta\rho_3$) to the deformation density ($\Delta\rho$) calculated from the *corresponding* NOCV pairs for *cis*-$W(CO)_4(piperidine)_2$ complex. The $|\Delta\rho|$=0.01 a.u. contours are shown

describes transfer of electron from the tungsten to the ligand (back-donation). The third pair of NOCV describes the donation (CO → metal). Thus, NOCV can be directly used in a discussion of bonding in terms of the 'classical' Dewar–Chatt–Duncanson model [44, 45]. The corresponding eigenvalues can be used as measures of the synergic electron transfer processes (Eq. 5): σ-donation can quantified by Δq_d=0.55, and the π-back-donation by $\Delta q_{bd} = 0.50 + 0.44$. It was shown [28–31] that Δq_d and Δq_{bd} are in qualitative agreement with other measures of donation/back donation processes, such as orbital interaction energy or changes in Mulliken electron populations of frontier orbitals.

For the $W(CO)_4(piperidine)_2$ complex, the values of Δq_d and Δq_{bd} (Table 1) calculated for the two metal-CO bonds ($C_{(3)}O_{(8)}$ and $C_{(4)}O_{(9)}$) show that both components are responsible for strengthening of the bond involving CO *trans* to piperidine. The backbonding component is larger in both cases, Δq_{bd} values are 1.09 and 0.94 for $C_{(3)}O_{(8)}$ and $C_{(4)}O_{(9)}$, respectively. The corresponding eigenvalues describing donation, Δq_d, are 0.65 and 0.55. Comparing the bonds involving the two carbonyl group, Δq_{bd} is increased for $C_{(3)}O_{(8)}$ by ca. 0.10, and Δq_{bd} by ca. 0.15.

Thus, the results of NOCV analysis show that the CO-metal bond in *trans* position to piperidine is stronger as a result of an increase in both components, σ-donation and π-backbonding. Accordingly the corresponding C–O bond is weakened. The results of this complementary analysis are consistent with the picture resulting from bond-orders and bond-energies.

Concluding remarks

In the present study we analyzed bond-orders, bond-energies, and bond-orbitals (NOCV's) describing the electronic structure of *cis*-$W(CO)_4(piperidine)_2$ complex. The main goal was to describe the bonding in the $W(CO)_4(piperidine)_2$ and its dimer. The results were discussed together with the experimental based picture drawing from vibrational ν_{CO} frequencies for *cis*-$W(CO)_4(piperidine)_2$ systems in the solid state [18]. The NOCV, bond-orders and bond-energies based results indicate that there exist noticeable differences in the metal-carbon and carbon-oxygen bonds involving the carbonyl groups positioned *trans* and *cis* to the piperidine ligand. Namely, the metal-carbon bond *trans* to piperidine is stronger, compared to that located in the *cis* position, as a result of an increase in both, the ligand metal → donation and metal → ligand π-back-bonding. Consequently, the carbon-oxygen bond within carbonyl group is already weakened in the monomeric complex. In the dimeric complex, modeling the interactions in the solid state, we find that the C–O bond involved in the inter-molecular hydrogen bonding is further weakened. This implies that C–O stretching frequencies should farther decrease in solid state. Indeed, this effect was noted by Braunstein et al. for this complex in the solid state, in which unusual low CO stretching frequencies was reported [18].

The results of the present study demonstrate as well the usefulness of the methodology applied here. A combination of bond-energy and bond-order analysis supported by NOCV gives a detailed description of various aspects of bonding, including the quantitative description of the 'classical' concepts of donation and back-donation.

References

1. Mond L, Quincke LC (1890) J Chem Soc 57:749–753
2. Cotton FA, Wilkinson G (1998) Advanced inorganic chemistry. Wiley, New York
3. Solomon EI, Lever ABP (2006) Inorganic electronic structure and spectroscopy. Wiley, New York
4. Elschenbroich C (2005) Organometallics. Wiley-VCH, Weinheim
5. Pruchnik F (1990) Organometallic chemistry of transition metal elements. Plenum, New-York
6. Werner H (1990) Angew Chem Int Ed 29:1077–1089
7. Cotton FA (1976) Prog Inorg Chem 21:1–28
8. Ellis JE, Beck W (1995) Angew Chem Int Ed 34:2489–2491
9. Davidson R (1993) Acc Chem Res 26:628–635
10. Frenking G, Fröhlich N (2000) Chem Rev 100:717–774 and refs therein
11. Ziegler T, Autschbach J (2005) Chem Rev 105:2695–2722 and refs therein
12. Ziegler T (1991) Chem Rev 91:651–667
13. Solomon EI, Jones PM, May JA (1993) Chem Rev 93:2623–2644
14. Sen A (2002) Catalytic synthesis of alkene—carbon monoxide copolymers and cooligomers. Kluwer Academic Publishers, Dordrecht
15. Cariati E, Roberto D, Ugo R (2003) Chem Rev 103:3707–3732
16. Ragsdale SW, Kumar M (1996) Chem Rev 96:2515–2539
17. Zhou M, Andrews L, Bauschlicher CW (2001) Chem Rev 101:1931–1961
18. Braunstein P, Taquet JP, Siri O, Welter R (2004) Angew Chem Int Ed 43:5922–5925
19. Nalewajski RF, Mrozek J (1994) Int J Quant Chem 51:187–200
20. Nalewajski RF, Mrozek J, Formosinho SJ, Varandas AJC (1994) Int J Quant Chem 52:1153–1176
21. Nalewajski RF, Mrozek J (1996) Int J Quant Chem 57:377–389
22. Nalewajski RF, Mrozek J, Mazur G (1996) Can J Chem 74:1121–1130
23. Nalewajski RF, Mrozek J, Michalak A (1997) Int J Quant Chem 61:589–601
24. Nalewajski RF, Mrozek J, Michalak A (1998) Polish J Chem 72:1779–1791
25. Michalak A, De Kock R, Ziegler T (2008) J Phys Chem A 112:7256–7263
26. Ziegler T, Rauk A (1978) Theor Chim Acta 46:1–9
27. Ziegler T, Rauk A (1979) Inorg Chem 18:1755–1759
28. Michalak A, Mitoraj M, Ziegler T (2008) J Phys Chem A 112:1933–1939
29. Mitoraj M, Michalak A (2007) Organomet 26:6576–6580
30. Mitoraj M, Michalak A (2007) J Mol Model 13:347–355
31. Mitoraj M, Michalak A (2008) J Mol Model 14:681–687

32. Mitoraj M, Zhu H, Michalak A, Ziegler (2008) Int J Quant Chem . doi:10.1002/qua.21910
33. Mitoraj M, Michalak A, Ziegler T (2009) J Chem Theor Comput 5:962–975
34. te Velde G, Bickelhaupt FM, Baerends EJ, Fonseca Guerra C, van Gisbergen SJA, Snijders JG, Ziegler T (2001) J Comput Chem 22:931–967 and refs therein
35. Baerends EJ, Ellis DE, Ros P (1973) Chem Phys 2:41–51
36. Boerrigter PM, te Velde G, Baerends EJ (1988) Int J Quantum Chem 33:87–113
37. Fonesca Geurra C, Visser O, Snijders JG, te Velde G, Baerends EJ (1995) In: Clementi E, Corongiu G (eds) Methods and techniques in computational chemistry METACC-9. STEF, Cagliari, pp 303–395
38. Becke A (1988) Phys Rev A 38:3098–3100
39. Perdew JP (1986) Phys Rev B 34:7406–7406
40. Perdew JP (1986) Phys Rev B 33:8822–8824
41. Ziegler T, Tschinke V, Baerends EJ, Snijders JG, Ravenek W (1989) J Phys Chem 93:3050–3056
42. Snijders JG, Baerends E (1978) Mol Phys 36:1789–1904
43. Snijders JG, Baerends EJ, Ros P (1979) Mol Phys 38:1909–1929
44. Dewar MJS (1951) Bull Soc Chim 18:C71–C79
45. Chatt J, Duncanson JA (1953) J Chem Soc 3:2939–2943